International Symposium
On Turbulence and Shear Flow
Phenomena (TSFP-9)
June 30 - July 3, 2015 *Melbourne, Australia*

CONVECTION OF MOMENTUM TRANSPORT EVENTS IN A TURBULENT BOUNDARY LAYER

Roeland de Kat
Engineering and the Environment
University of Southampton
Tizard, Highfield, Southampton, SO17 1BJ, UK
r.de-kat@soton.ac.uk

Bharathram Ganapathisubramani
Engineering and the Environment
University of Southampton
Tizard, Highfield, Southampton, SO17 1BJ, UK
g.bharath@soton.ac.uk

INTRODUCTION

Understanding momentum events in turbulent boundary layers is of crucial importance for modelling and controlling turbulent wall-flows. A lot of effort is put into capturing, characterising, and quantifying the instantaneous and statistical properties of structures responsible for momentum transport in wall-bounded turbulent flow: e.g. Katul *et al.* (2006) show the relative importance of ejections and sweeps in an atmospheric boundary layer, Adrian (2007) describes the organisation of hairpin vortices in wall turbulence, Dennis & Nickels (2011*a*,*b*) show vortex packets and long structures in a turbulent boundary layer, and Lozano-Durán *et al.* (2012) characterises the three-dimensional structure of momentum transport in turbulent channels.

Balakumar & Adrian (2007) indicate that more than 40% of the total shear-stress in turbulent boundary layers is related to scales larger than three boundary layer thicknesses (3δ). Large regions of low- or high-momentum relate to the organisation of vortical structures Adrian (2007). Large scale velocity fluctuations modulate the amplitude and frequency of smaller scales (Ganapathisubramani *et al.*, 2012; de Kat & Ganapathisubramani, 2013). Lee & Sung (2011) link vortex heads and shear layers in a turbulent boundary layer to ejection and sweep events. Lee *et al.* (2014) investigate the evolution of the streamwise velocity of very-large- and large-scale motions and find that low-speed regions convect slower than the local mean and high-speed regions faster. Elsinga *et al.* (2012) track vortices and find that they travel at a velocity closer to the local centroid velocity than to the mean velocity. Lozano-Durán & Jiménez (2014) show the structure, evolution and motion of momentum transport events in a turbulent channel flow. However, the convection of ejection and sweep events in a turbulent boundary layer has not yet been covered.

In this study, we evaluate the convection of momentum transport events from time-resolved particle image velocimetry (PIV) data in a stream-wise wall-normal plane of a turbulent boundary layer.

EXPERIMENT

Time-resolved PIV experiments are performed in a stream-wise wall-normal plane in a turbulent boundary layer in the water tunnel at Cambridge University Engineering Department. The flow is tripped with a glass rod at the beginning of the test-section and PIV measurements are performed 4–5 m downstream of this trip. The nominal flow conditions at the measurement location are $U \approx 0.65$ m/s, $\delta \approx 0.1$ m, $U_\tau \approx 0.027$ m/s, and $Re_\tau \approx 2700$. Particle image pairs are captured and processed using LaVision software DaVis 7.2. The experiment has a field-of-view that covers an area of 17 $\times$ 4.5 cm (approximately 2 δ $\times$ 0.5 δ) with a digital resolution of 22 pixels/mm and a total of 50,000 images are acquired in 10 separate sets at 1 kHz, covering 50 s of flow. Images are preprocessed using a min-max normalisation. Gaussian weighted correlation starts with an initial effective window size (WS) of 64 by 64 pixel and finishes at 16 by 16 pixels with an overlap factor of 50%. This results in a spatial resolution of $\Delta x^+ = 10$ ($l^+ = 20$, WS = 0.7 mm) with a temporal resolution of $\Delta t^+ = 0.7$.

MOMENTUM TRANSPORT EVENTS

Momentum transport events are analysed using a quadrant decomposition and are divided into four quadrants (Q1-Q4). The dominant quadrants in turbulent boundary layers are Q2, ejections, and Q4, sweeps (e.g. Katul *et al.*, 2006), meaning that low momentum fluid is moved away from the wall and high momentum fluid is moved towards the wall.

We use a hole analysis Willmarth & Lu (1972) with respect to the maximum shear in the boundary layer to restrict ourselves to look at stronger events. The hole analysis only takes events stronger than a threshold into account determined by equation 1.

$$u'v' > H\,\overline{u'v'}\big|_{\max} \tag{1}$$

where $u'v'$ is the instantaneous shear-stress, H the hole size, and $\overline{u'v'}\big|_{\max}$ the maximum mean shear-stress.

Before applying the hole analysis, we filter the data with a 2D Hanning filter with a linear full-width-at-half-max of 0.028δ to remove small features that would overwhelm feature detection. Most of the momentum transport takes place at larger scales (Balakumar & Adrian, 2007) and after filtering 93% of the total stress within the field of view is captured, which shows that the filtering will not influence our results significantly. Applying threshold of $H = 2$ results in a total of 77% of the total stress captured. Momentum transport events are identified by capturing the outline of $H = 2$ regions and categorising them by their quadrant. Weighted centroid, area, contribution to shear and bounding box of the events are determined.

Figure 1 shows two examples of resulting negative shear-stress events, Q^-s. These examples show occasions where both sweep and ejection events are present within the field-of-view.

RESULTS & DISCUSSION

Size and contribution to shear

To understand what size of momentum transport event is important to follow, we take weighted probability functions to determine the (relative) contribution to the total momentum transport (shear-stress) within our field-of-view.

First, we look at the contribution that different area sizes have. Figure 2*left* shows the relative contribution to momentum transport within our field-of-view. The range of areas covered by ejections and sweep is the same, however, the ejections contribute more to the shear-stress for all area sizes. This indicates that (on average) ejection events of the same area will be stronger than sweep events. Due to this difference in strength, the area of median contribution to the shear-stress is $0.049\delta^2$ for ejections and $0.043\delta^2$ for sweeps. The other two quadrants show a smaller range of areas and have a significantly lower contribution to the shear-stress. Interestingly, Q1 has a larger contribution than Q3, suggesting that events that have a wall-normal component away from the wall dominate.

Second, we look at the bounding box of the events. Figure 2*right* shows the bounding box size in streamwise Δx and wall-normal Δy direction for ejections (top) and sweeps (bottom). Contribution to shear of ejections extend further in streamwise direction, supported by a 14% increase in median contribution size from 0.30δ to 0.34δ. This difference causes the difference in median contribution area, because the wall-normal size remain very similar and change less than 3%.

Convection trajectories

The momentum transport events will move in both wall-normal and streamwise direction. To get an impression of the wall-normal motion, we can look at the time history of centroids leading up to the time depicted in figure 1, and these time tracks are shown in figure 3. We can see that both ejections and sweeps have a range displacement in wall-normal direction for their trajectories. Most sweep events appear to move downward, whereas most ejection event appear to move upwards. However, especially in areas where they interact (are close together), they appear to remain level or move in the opposite direction.

To get an impression of the streamwise motion, we take a look at the centroid evolution in the x–t-plane (ignoring the wall-normal locations for now), figure 4. All centroid trajectories appear to move in streamwise direction in time, consistent with the flow moving from left to right. However, closer inspection reveals that the sweeps and ejections show different slopes in this x–t-plane, indicating different convection velocities.

Convection velocities

To determine and quantify the motion of the sweeps and ejections we will look at probability density functions (p.d.f.'s) of convection velocity. By evaluating singly-connected events, de Kat & Ganapathisubramani (2014) found that ejections tended to move up faster than sweeps move down and that sweeps convect faster in streamwise direction than ejections. However, they looked at these singly-connected events over a $\Delta t^+ \approx 0.7$, which resulted in broad p.d.f.'s of convection velocity due to the influence of measurement noise over such a small time separation. To reduce the influence of measurement noise we will look at the average convection velocities of events that are connected in time and space. We first evaluate all the events that are connected—in time and space—in graphs, similar to Lozano-Durán & Jiménez (2014). Next, the graph centroid at each time-step is determined and its evolution in time gives us the convection velocity in streamwise and wall-normal direction. Then, the average convection velocity of each graph is determined, graphs with a time-span of $\Delta t^+ < 30$ are removed, resulting in a total of 1653 ejections graphs and 1629 sweep graphs. To account for difference in the streamwise flow velocity with wall-normal distance, these events are binned into 30 bins—spanning all wall-normal locations—based on the wall-normal location of the graph's time-averaged centroid. Finally, p.d.f.'s of convection velocities are determined.

For the wall-normal motion, Lozano-Durán & Jiménez (2014) found that in their turbulent channel flow simulations, ejections and sweeps move at approximately the skin friction velocity, U_τ—up and down, respectively. In our turbulent boundary layer experiment, we find that ejections and sweeps move at different wall-normal velocities, figure 5*left*. Ejections move up at 0.5 U_τ and sweeps move down at 0.25 U_τ (based on average and median convection velocities). Unlike a turbulent channel flow, a turbulent boundary layer is not restricted in height and will therefore grow. The asymmetry in the convection velocities may be related to this growth. Despite the difference in magnitude between different flows, positive wall-normal velocity fluctuations—on average—move up and negative ones move down.

The streamwise motion of velocity fluctuations has received more attention than the wall-normal location, and our results show that positive streamwise velocity fluctuations move faster than negative streamwise velocity fluctuations at all wall-normal locations, see figure 5*right*. They appear symmetric around the local mean velocity. This corroborates the results in channel flow (see Lozano-Durán & Jiménez, 2014), where for similar wall-normal locations the fluctuations display a symmetric streamwise-convection-velocity-distribution around the local mean velocity for sweeps and ejections. Buxton *et al.* (2013) show that the dependency of streamwise-convection-velocity on the sign of the streamwise velocity fluctuation is also present in turbulent mixing layers. This shows that across different flows, positive streamwise velocity fluctuations move faster than negative streamwise velocity fluctuations and the local mean velocity lies in between them.

CONCLUSIONS

In this study, we evaluated the convection of momentum transport events from time-resolved particle image velocimetry data in a stream-wise wall-normal plane of a turbulent boundary layer. Our data shows that ejections move up twice as fast as sweeps move down and the magnitude of both is less than that observed in simulations of turbulent channel flow. Despite the difference in magnitude between different flows, positive wall-normal velocity fluctuations—on average—move up and negative ones move down. Sweeps move faster in streamwise direction than the local mean and ejections move slower. Across different flows, positive streamwise velocity fluctuations move faster than negative streamwise velocity fluctuations and, generally, the local mean velocity lies in between them.

ACKNOWLEDGEMENT

The research leading to these results has received funding from the European Research Council under the European Union's Seventh Framework Programme (FP7/2007-2013) / ERC Grant agreement no 277472-WBT

REFERENCES

Adrian, R. J. 2007 Hairpin vortex organization in wall turbulence. *Phys. Fluids* **19**, 041301.

Balakumar, B. J. & Adrian, R. J. 2007 Large- and very-large-scale motions in channel and boundary-layer flows. *Phil. Trans. R. Soc. A* **365**, 665–681.

Buxton, O. H. R., de Kat, R. & Ganapathisubramani, B. 2013 The convection of large and intermediate scale fluctuations in a turbulent mixing layer. *Phys. Fluids* **25**, 125105.

Dennis, D. J. C. & Nickels, T. B. 2011*a* Experimental measurement of large-scale three-dimensional structures in a turbulent boundary layer. part1. vortex packets. *J. Fluid Mech.* **673**, 180–217.

Dennis, D. J. C. & Nickels, T. B. 2011*b* Experimental measurement of large-scale three-dimensional structures in a turbulent boundary layer. part2. long structures. *J. Fluid Mech.* **673**, 218–244.

Elsinga, G. E., Poelma, C., Schöder, A., Geisler, R., Scarano, F. & Westerweel, J. 2012 Tracking of vortices in a turbulent boundary layer. *J. Fluid Mech.* **697**, 273–295.

Ganapathisubramani, B., Hutchins, N., Monty, J. P., Chung, D. & Marusic, I. 2012 Amplitude and frequency modulation in wall turbulence. *J. Fluid Mech.* **712**, 61–91.

de Kat, R. & Ganapathisubramani, B. 2013 Characteristics of Reynolds stresses in a turbulent boundary layer. In *Int. Symp. On Tubulence and Shear Flow Phenomena, TSFP-8*.

de Kat, R. & Ganapathisubramani, B. 2014 Convection of momentum transport events in a turbulent boundary layer. *Bulletin of the American Physical Society* **59**.

Katul, G., Poggi, D., Cava, D. & Finnigan, J. 2006 The relative importance of ejections and sweeps to momentum transfer in the atmospheric boundary layer. *Boundary-Layer Meorol.* **120**, 367–375.

Lee, J., Lee, J. H., Choi, J.-I. & Sung, H. J. 2014 Spatial organization of large- and very-large-scale motions in a turbulent channel flow. *J. Fluid Mech.* **749**, 818–840.

Lee, J. H. & Sung, H. J. 2011 Very-large-scale motions in a turbulent boundary layer. *J. Fluid Mech.* **673**, 80–120.

Lozano-Durán, A., Flores, O. & Jiménez, J. 2012 The three-dimensional structure of momentum transfer in turbulent channels. *J. Fluid Mech.* **694**, 100–130.

Lozano-Durán, A. & Jiménez, J. 2014 Time-resolved evolution of coherent structures in turbulent channels: characterization of eddies and cascades. *J. Fluid Mech.* **759**, 432–471.

Willmarth, W. W. & Lu, S. S. 1972 Structure of the Reynolds stress near the wall. *J. Fluid Mech.* **55**, 65–92.

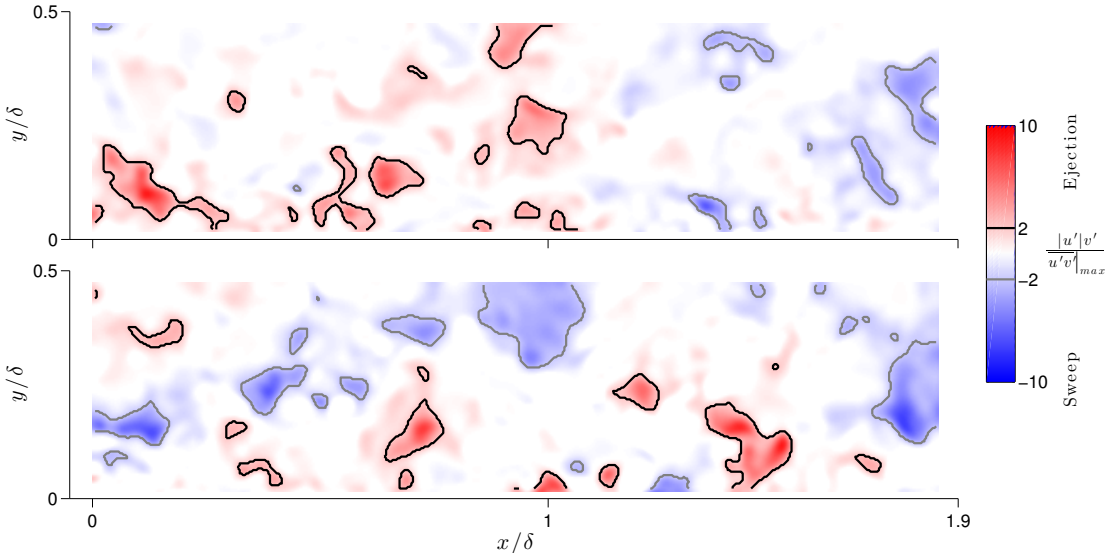

Figure 1. Examples of Q^- momentum transport events. Boundaries of areas for a hole size $H = 2$ are indicated by lines.

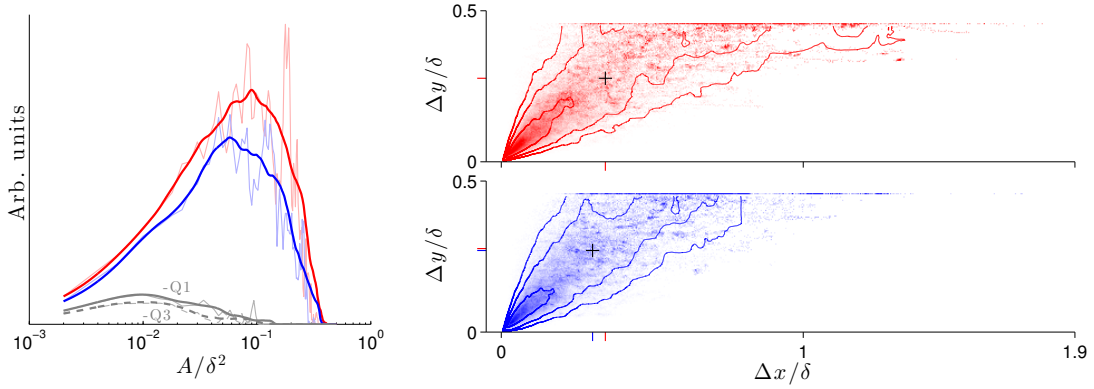

Figure 2. Relative contribution to shear for $H = 2$, statistics of area and bounding box of momentum transport events. *Left*: Contribution per area size A. area in the plot equals contribution. Filtered *solid* and unfiltered results in *shaded* colour. *Right*: Contribution per streamwise Δx and wall-normal Δy bounding box size. Filtered results *solid* contours and unfiltered results background *shades*. Cross indicates median contribution.

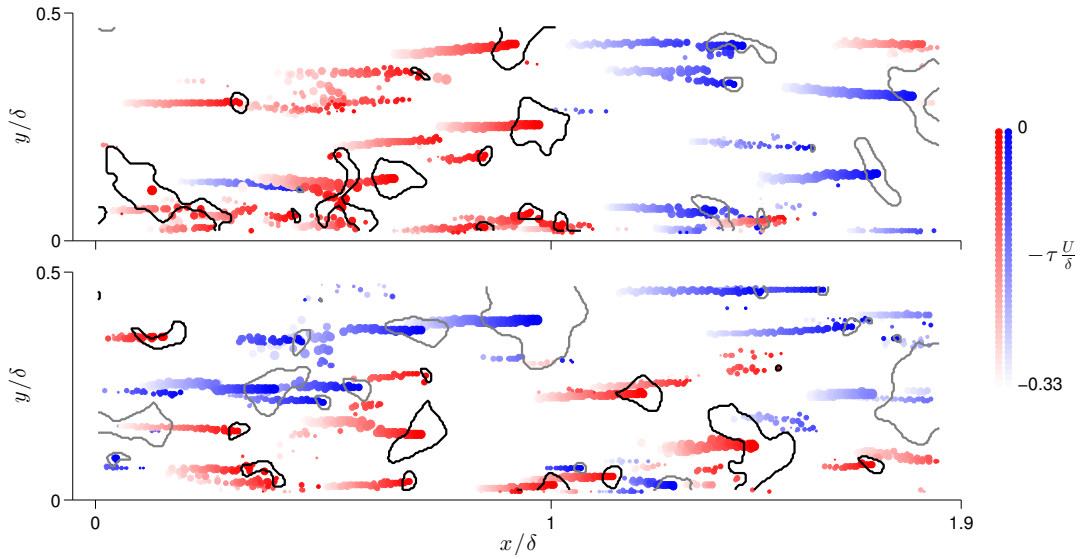

Figure 3. Examples of Q^- momentum transport event convection in a streamwise–wallnormal plane—x–y plane. Centroid path history for $t-\tau$ leading to the events in figure 1 is indicated by coloured dots. Dot size is indicative of the area of the event. Centroids of events entering or exiting the field-of-view in streamwise direction have been omitted.

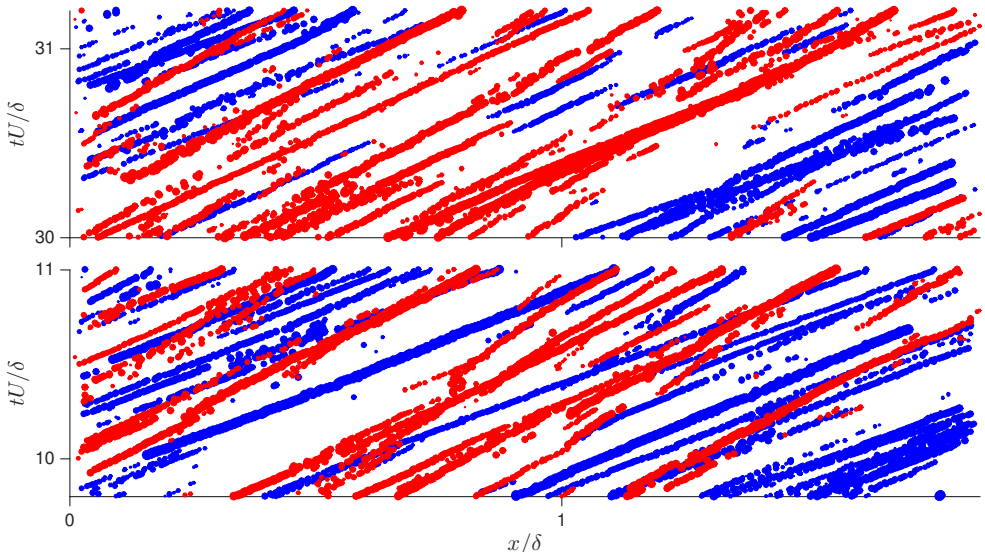

Figure 4. Examples of Q^- momentum transport event convection in the streamwise–time plane—x–t plane. All y-locations are included. Dot size is indicative of the area of the event. Centroids of events entering or exiting the field-of-view in streamwise direction have been omitted.

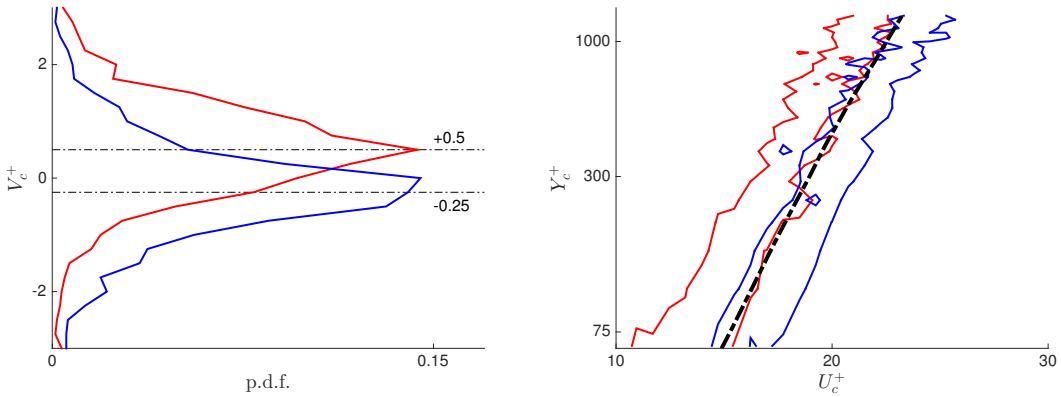

Figure 5. Probability density functions of wall-normal and streamwise convection velocity of Q^- moment transport events. *Left* Wall-normal convection velocity. *Right* Stream-wise convection velocity with wall-normal location. Contours show 50% of the peak at each wall-normal location. The thick *dash-dotted* line indicate the local mean velocity.